CIVIL ENGINEERING JOURNAL

Article no. 5

THE CIVIL ENGINEERING JOURNAL 1-2024

STUDY ON CONSTRUCTION MONITORING AND CONTROL OF MULTI-SPAN PRESTRESSED CONCRETE CONTINUOUS BEAM BRIDGE

Xilong Zheng and Di Guan

School of Civil and Architectural Engineering, Harbin University, No.109 Zhongxing Road, Harbin, Heilongjiang Province, China; sampson88@126.com

ABSTRACT

This article focuses on the construction monitoring and control of a pre-stressed concrete continuous beam bridge, consisting of 13 spans. The goal is to ensure that the bridge structure meets the design requirements throughout the entire construction process. By comparing the theoretical and measured values of the bridge's alignment and stress during the cantilever construction, closure, and completion phases, it can be observed that the deflection deformation of the bridge is generally in agreement with the theoretical calculations. After the completion of the entire bridge, the measured elevations of each section have an error range of -18mm to 20mm compared to the design elevations, which satisfies the specifications. A comparison analysis of the measured and theoretical stress values at the root and mid-span of the cantilever indicates that the stress difference at the root is within the range of -0.2MPa to 0.2MPa, and the stress differences at the mid-span after completion are 0.03MPa (upper) and 0.09MPa (lower), all of which meet the structural design and code requirements. By establishing a gray GM (1,1) model and using gray system theory, the deflection error during the construction process is predicted and controlled. The prediction accuracy of different methods is compared to determine a reasonable prediction method suitable for long-span pre-stressed continuous beam bridges, providing reference for similar engineering projects.

KEYWORDS

Long-span bridge, Continuous beam bridge, Grey system theory, Construction control

INTRODUCTION

A continuous beam bridge refers to a beam bridge with two or more continuous spans, belonging to a statically indeterminate system. Under the effect of constant and live loads on a continuous beam bridge, the negative bending moment at the supports can relieve the positive bending moment at the mid-span, resulting in a more uniform and rational internal force distribution. Therefore, continuous beam bridges have advantages such as reduced height, material savings, high stiffness, good overall performance, high overload capacity, high safety, and low cost. Pre-stressed concrete continuous beam bridges are a type of pre-stressed bridge that offers advantages such as good overall performance, high structural stiffness, minimal deformation, and good seismic performance. In particular, the deflection curve of the main beam is smooth, with small deformation and comfortable driving conditions [1-3]. Furthermore, the design and construction of this type of bridge are relatively mature, ensuring control over construction quality and duration, and requiring less maintenance after completion. These factors have led to the widespread application of such bridges in highway, urban, and railway bridge projects [4-6].

The development of continuous beam bridges saw significant progress in the 1950s when pre-stressed concrete surpassed spans of 100 meters. By the 1980s, spans even exceeded 440

meters. Conventional reinforced concrete structures had several drawbacks, such as premature cracking, inability to effectively utilize high-strength materials, high structural weight, and poor load-carrying capacity, resulting in low material efficiency. To address these issues, pre-stressed concrete structures emerged. Since the mid-20th century, with the construction of the Rhein River cantilever casting bridge in Germany, cantilever casting and cantilever assembly construction methods have been improved, refined, and widely adopted worldwide for pre-stressed concrete continuous beam bridges [7-10]. However, the diversification of bridge structures and the continuous increase in span lengths have presented greater challenges in bridge design, construction, and management. While promoting the development of related industries, ensuring the structural safety of bridges has become a crucial concern for construction managers [11-13]. Ensuring structural safety has become an indispensable part of the bridge construction process. Consequently, bridge construction control technology has become a popular research topic. It involves identifying influential parameters, determining key factors, and providing reasonable guidance for bridge construction through error analysis and adjustment [14-16].

Ye Zaijun [17] used the grey system theory and established a GM(1,1) prediction model to predict the elevation errors of the beam segment box beams during the cantilever pouring process of the Danjiangkou Bridge in the South-to-North Water Diversion Project. This allowed for adjustments to be made to the subsequent construction process based on the predicted errors. The application of the grey system theory in this predictive model is a common and effective method in engineering construction. Qu Guangzhen [18] conducted a study on the effects of system transformation and shrinkage on the elevation and stress of the bridge, using the Wuhan-Jingmen High-speed Railway Hanjiang Extra-large Bridge as the background. Additionally, this study analyzed the impact of other parameter errors and the closure sequence on the structure, aiming to reduce construction errors. Zhou Langfeng [19] conducted a simulation analysis of the entire construction process of the Hanjiang Extra-large Bridge in the Wuhan-Jingmen High-speed Railway project. This study analyzed the effects of concrete shrinkage and creep on the bridge's alignment and investigated the impact of temperature on structural deformation and stress. These analyses ensured the control of elevation and stress during the closure process.

This paper takes a prestressed concrete continuous beam bridge as the engineering background, with a specific main bridge as a 13-span continuous system. The study focuses on monitoring the alignment and stress during the bridge construction process. The grey system theory is applied to predict and control the deflection error during construction, ensuring that the structure meets the design requirements throughout the entire construction process.

BACKGROUND

This paper takes a dual-purpose road-rail bridge in Fujian province, with a total length of 3713.475m, as the engineering background. The main bridge is a 13-span continuous variable-section box girder, with span arrangements of 40m + 11×64m + 40m, and a total length of 784m, as shown in Figure 1. The superstructure adopts a single-box single-cell variable-section prestressed continuous box girder. The beam body has a single-box single-cell, variable-section, and variable-height structure. The top width of the box girder is 17.5m. The inclined diaphragm and the height of each control section beam are as follows: 2.8m at the end support and mid-span, and 4m at the mid-support, with a varying height in accordance with a circular curve. The bridge deck is set as a dual carriageway with a total width of 35.5m. The width of the left and right carriageways is both 17.5m, with a 0.5m gap in the middle. The transverse layout includes: 1.25m (guardrail and water pipe) + 0.5m (anti-collision wall) + 3.0m (hard shoulder) + 11.25m (driving lane) + 0.75m (road shoulder) + 2.0m (central separator) + 0.75m (road shoulder) + 11.25m (driving lane) + 3.0m (hard shoulder) + 0.5m (anti-collision wall) + 1.25m (guardrail and water pipe), totalling 35.5m. The elevation view of the main bridge is shown in Figure 2.

Fig. 1 – The main bridge of a dual-purpose road-rail bridge in Fujian province

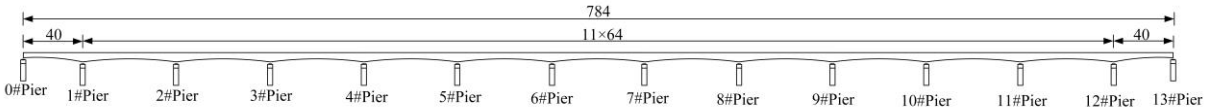

Fig. 2 – Elevation view of the main bridge (unit: m)

The box girder adopts C55 high-performance concrete, the pier and abutment body adopt C50 concrete, the fill concrete for pier and abutment adopts C20 concrete, and the foundation adopts C40 concrete. The prestressing of the box girder is done using low relaxation high-strength prestressing steel strands with a nominal area of 140mm2, a nominal diameter of 15.2mm, an elastic modulus of 1.95×105MPa, and a standard tensile strength of 1860MPa. The anchoring system uses wedge anchorage, and the drilling is done using metal corrugated pipes.

The vertical prestressing bars use prestressed threaded steel reinforcement, with the model JL785. The standard tensile strength of the prestressing steel reinforcement for prestressed concrete is 785MPa, and the controlled stress under anchorage is 650MPa. The prefabricated holes are φ35 with iron skin. During construction, a two-stage tensioning process is used, and the anchorage device should not have a retraction greater than 1mm. The ordinary reinforcement uses smooth round steel bars HPB300 and ribbed steel bars HRB400.

ESTABLISHMENT OF FINITE ELEMENT MODEL

The main bridge is primarily modelled and analyzed using the Midas/Civil finite element software. The finite element model of the entire bridge is shown in Figure 3. Since the longitudinal and transverse arrangements of the two spans of the bridge are completely identical, calculations are only performed on a single span bridge model. The upper structure of the entire bridge is divided into 262 nodes and 261 elements. Considering the construction sequence and the effects of shrinkage and creep, the structural analysis is conducted using the positive-loading method.

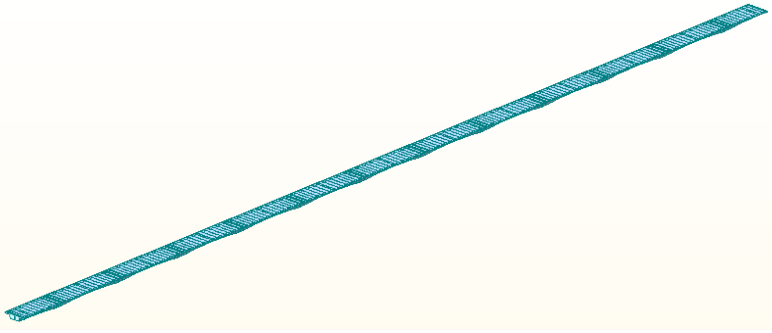

Fig. 3 – Midas/Civil finite element model diagram

The entire bridge consists of 13 spans, and during the cantilever casting construction process, it is divided into 12 T-segments. Each T-segment has a maximum cantilever state divided into 8 casting segments for cantilever casting. The casting segments for smaller distances are represented as 0'#~7'#, while the casting segments for longer distances are represented as 0#~7#. The division of T-segment beams is shown in Figure 4.

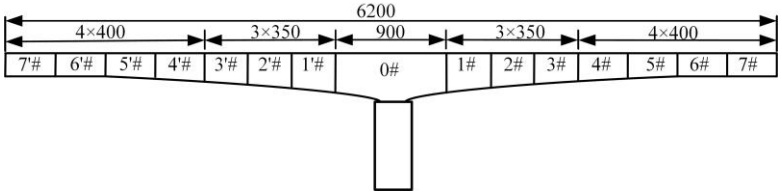

Fig. 4 – Cantilever construction beam segment division diagram (cm)

ARRANGEMENT OF CONSTRUCTION MONITORING POINTS

The main monitoring contents during the construction process include the following points:

(1) Deflection observation: Perform periodic levelling measurements on the top observation points of the box girder according to the construction process (before and after pouring, before and after prestressing, before and after basket hanging).

(2) Stress observation: Perform stress measurements on the embedded components installed inside the box girder.

Deflection observation

The main content of deflection observation is to measure the elevation of each cast-in-place segment of the box girder to determine if the bridge alignment and elevation match the design. Three symmetrical elevation observation points are set up at each construction stage to measure the deflection of the box girder and observe if any torsion occurs. The specific process involves measurements by the construction unit, verification by the supervision unit, and then compilation and processing by the monitoring unit. The measurement points are shown in Figure 5.

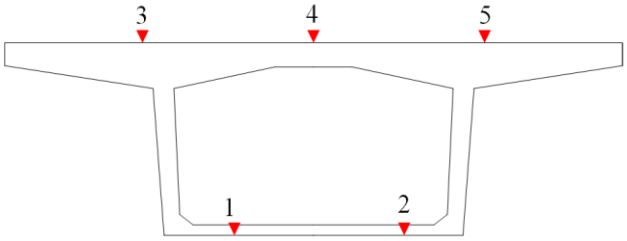

Fig. 5 – Elevation measurement point layout diagram for formwork

Stress observation

According to the characteristics and requirements of this project, different stress monitoring positions are selected. Four measurement points are arranged on each main beam stress testing section. One measurement point is arranged on each temporary fixed support on the top of each pier. Three sling measurement points are arranged on each hanging basket. The layout of main beam measurement points is shown in Figure 6 and Figure 7, using embedded concrete strain gauges with temperature sensors. The strain sensors should be fixed on the steel reinforcement frame before concrete pouring, and the test wires should be led into the box and properly marked and protected. According to the actual construction process, a total of four measurements are conducted for each segment during construction: before and after concrete pouring, before and after pre-stressing, and stress-strain monitoring should also be carried out after main beam closure and completion of phase two permanent loading construction.

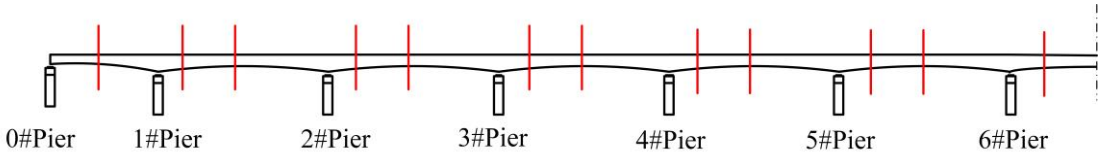

Fig. 6 – Layout diagram of stress testing sections for Continuous Beam 1/2

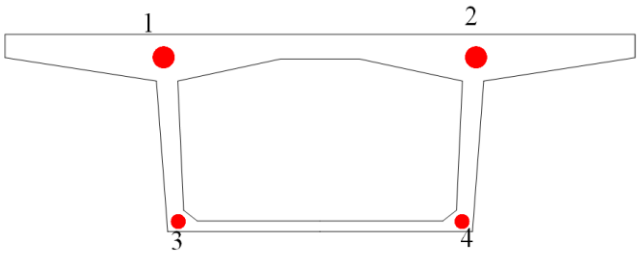

Fig. 7 – Layout diagram of stress measurement points

CONSTRUCTION MONITORING AND CONTROL

Linear monitoring

The main task of linear control is to collect real-time measurement data during the actual construction process, compare the measured deflection variations with the finite element model, analyze, identify, and adjust the discrepancies between the two, and provide feedback to the model. By adjusting the model, it predicts the future state of the structure reasonably, ensuring a smooth alignment. Bridge alignment monitoring primarily includes three main stages: cantilever construction stage, final closure stage for each span, and the ultimate bridge completion stage.

Alignment control results during the cantilever casting stage

Due to the large number of spans in this project and the similarity of each structure during the cantilever construction stage, we only analyze the cantilever casting process of Pier 2. We compare the measured deflection changes of each beam section with the theoretical calculation deflection during the concrete casting, prestressing, and basket movement processes. Sections 0'# to 7'# represent short-distance beam sections, while sections 0# to 7# represent long-distance beam sections. The difference is calculated as the measured value minus the theoretical value. The deflection variations at each construction stage of Pier 2 during the entire construction process are shown in Figure 8 to Figure 10.

From the above analysis, it can be observed that during the cantilever construction process of Pier 2#, the deflection errors caused by concrete casting range from -1.29mm to 0.56mm, the errors due to prestressing range from -0.74mm to 1.32mm, and the errors caused by basket movement range from -0.49mm to 0.13mm. The deflection variations of each beam section are comparable to the theoretical deflection variations, meeting the accuracy requirements of alignment monitoring. The monitoring during the cantilever stage has achieved good results.

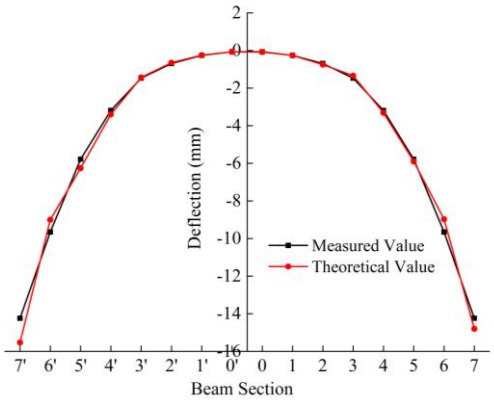

Fig. 8 – The diagram showing the variation of deflection in concrete pouring

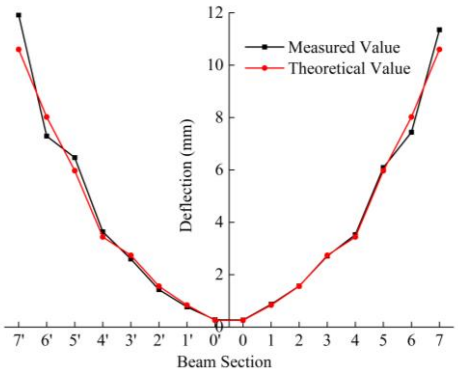

Fig. 9 – The diagram showing the variation of deflection in prestressed concrete

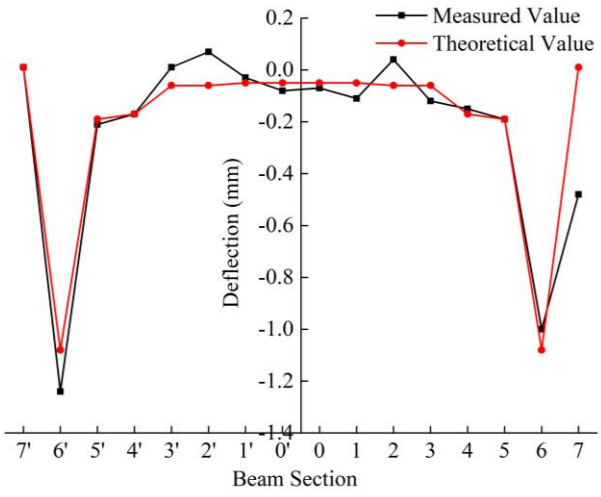

Fig. 10 – The diagram showing the variation of deflection in suspended scaffolding movement

The control results during the bridge closure stage

Due to the complexity of the bridge closure process and the involvement of multiple system conversion processes, this study focuses on the case of the closure of span 3# between pier 2# and pier 3# to analyze the monitoring results and the influence of closure on the deflection of span 3 at various points. Through analysis, the deflection effects of the closure of span 3 are shown in Figure 11 to Figure 13. It can be observed that during the closure of span 3, the deflection errors caused by concrete pouring range from -0.14mm to 0.1mm, the errors caused by prestressing range from -1.77mm to 2.56mm, and the errors caused by the removal of suspended scaffolding range from -0.69mm to 0.52mm. The deflection changes in each beam segment are similar to the theoretical deflection changes, meeting the accuracy requirements of linearity monitoring. The monitoring during the cantilever stage has achieved good results.

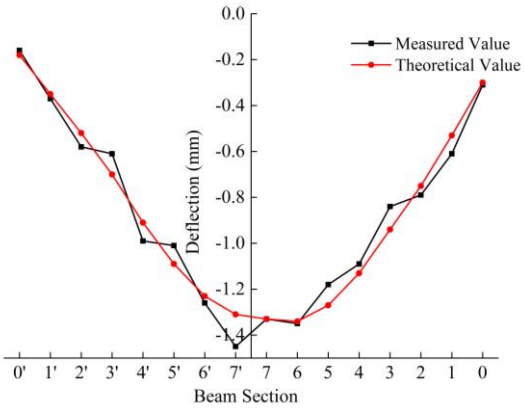

Fig. 11 – The deflection variation of the main beam during the concrete pouring in the bridge closure section

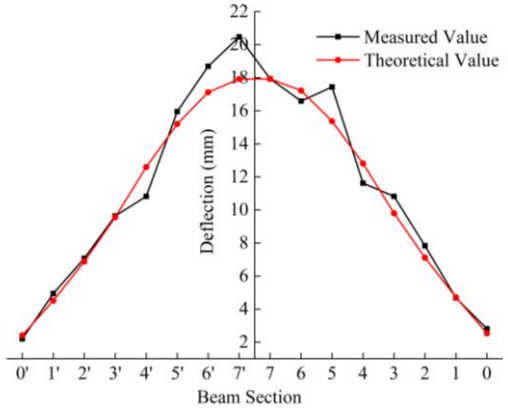

Fig. 12 –The deflection variation of the main beam during the prestressing in the bridge closure section

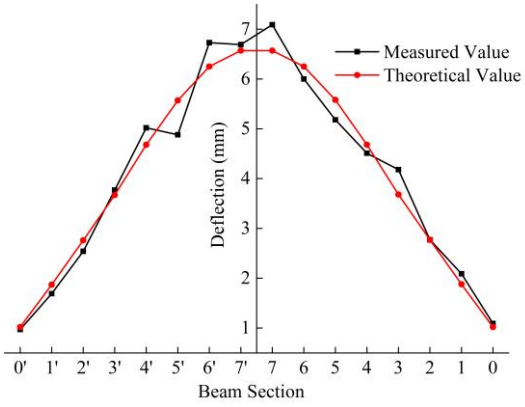

Fig. 13 – The deflection variation of the main beam during the removal of suspended scaffolding in the bridge closure section

The overall bridge closure line condition

The evaluation of whether the bridge alignment meets the design requirements after the completion of bridge closure in each span is an important criterion for judging the effectiveness of construction monitoring. Due to the long total span of the bridge, we can evaluate the monitoring results by comparing the measured elevations with the theoretical elevations, taking the span 3# between pier 2# and pier 3# as an example. The comparison between the measured elevations and the theoretical elevations at the control section of span 3# is shown in Table 1. From Table 1, it can be seen that the measured elevation values of each beam segment are in good agreement with the design elevation values, with errors ranging from -18mm to 20mm, which are within the specified requirements. The construction control of the project has achieved good results in terms of alignment.

Tab.1 - Alignment control effectiveness of Span 3 (m)

Beam segment	Theoretical elevation	Measured elevation	Difference
0'	48.123	48.125	0.002
1'	48.081	48.098	0.017
2'	48.039	48.045	0.006
3'	47.998	47.995	-0.003
4'	47.951	47.965	0.014
5'	47.906	47.903	-0.003
6'	47.862	47.843	-0.019
7'	47.819	47.825	0.006
7	47.808	47.815	0.007
6	47.797	47.783	-0.014
5	47.756	47.740	-0.016
4	47.715	47.725	0.010
3	47.676	47.696	0.020
2	47.638	47.640	0.002
1	47.605	47.587	-0.018
0	47.573	47.587	0.014

Cantilever construction process deflection prediction analysis

Comparison of different prediction methods

According to the characteristics of continuous beam bridge construction with long-term prestressing, the grey system theory is chosen to predict the deflection error. The cantilever pouring process of this project is regarded as a grey system, and the prediction of the adjustment value of pre-camber during the structural construction process is conducted. In order to demonstrate the reliability of the grey system prediction method, a comparative analysis is carried out between the grey system, BP neural network, and least squares method for predicting the elevation of the pouring process for the 5# to 7# beam segments at the 2# pier. The prediction errors are calculated using the three methods, and the results are shown in Table 2. The comparative analysis is illustrated in Figure 14.

Tab.2 - Comparison table of results from different prediction methods (mm)

Beam segment	Measured error value	Grey prediction value	BP prediction value	Least squares prediction value
5#	10.7	9.97	9.8	13.4
6#	8.5	8.71	8.7	7.8
7#	6.3	5.67	6.44	5

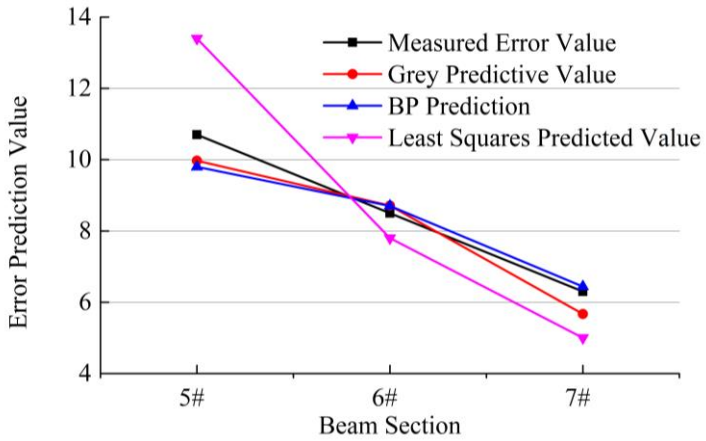

Fig. 14 – Comparison chart of three prediction values

According to Table 3 and Figure 14, it can be observed that the three prediction methods exhibit similar trends in predicting errors as the actual error development. All of them can effectively adjust the influence of construction errors in the project. Among the three prediction methods, the maximum error of grey prediction is 10.0%, the maximum error of BP neural network prediction is 9.03%, and the maximum error of least squares method is 27.55%. Both grey system theory and BP neural network prediction accuracy meet the requirements, and they can be regarded as effective methods for predicting the elevation of continuous beam bridges.

Stress monitoring results

Due to being a 13-span prestressed concrete continuous beam bridge, there are a total of 24 stress monitoring sections, and 4 monitoring points are required for each construction process in each segment, resulting in a large amount of data. Therefore, this study only compares the root of the cantilever at the far end of Pier 2# and the mid-span section of Span 2# at different construction stages. These two parts are divided into different construction stages for monitoring, as shown in Table 3.

Tab.3 - Construction stage division

Root of cantilever at Pier 2#				Mid-span of Span 2#	
Numbering	Construction phase	Numbering	Construction phase	Numbering	Construction phase
1	Pouring of Block 0#	16	Post-tensioning of Block 7#	1	Closure of Span 2# and Span 4#
2	Post-tensioning of Block 0#	17	Closure of Span 2# and Span 4#	2	Pouring of Segment 8# in Span 1#
3	Pouring of Block 1#	18	Pouring of Segment 8# in Span 1#	3	Closure of Span 3#
4	Post-tensioning of Block 1#	19	Closure of Span 3#	4	Closure of Span 6#
5	Pouring of Block 2#	20	Closure of Span 6#	5	Closure of Span 8#
6	Post-tensioning of Block 2#	21	Closure of Span 8#	6	Closure of Span 7#
7	Pouring of Block 3#	22	Closure of Span 7#	7	Closure of Span 5#
8	Post-tensioning of Block 3#	23	Closure of Span 5#	8	Closure of Span 10# and Span 12#
9	Pouring of Block 4#	24	Closure of Span 10# and Span 12#	9	Pouring of Segment 8# in Span 13#
10	Post-tensioning of Block 4#	25	Pouring of Segment 8# in Span 13#	10	Closure of Span 11#
11	Pouring of Block 5#	26	Closure of Span 11#	11	Closure of Span 9#
12	Post-tensioning of Block 5#	27	Closure of Span 9#	12	Closure of the side span
13	Pouring of Block 6#	28	Closure of the side span	13	Phase 2 pavement
14	Post-tensioning of Block 6#	29	Phase 2 pavement		
15	Pouring of Block 7#				

Monitoring results of stress at the root of the cantilever

The comparative analysis of Figure 15 and Figure 16 shows that during the entire cantilever pouring process, no tensile stress was observed at the root of the cantilever. The stress values continuously increased as the construction stages progressed, and the stress trend matched the actual conditions. The theoretical calculated values were generally consistent with the measured values, with a margin of error ranging from -0.2MPa to 0.2MPa, meeting the specifications requirements. The structural calculation model was reasonable, and the calculated results were accurate, providing guidance for the project. After the pouring was completed, the maximum stress at the upper edge of the cantilever root was 7.82MPa, and the maximum stress at the lower edge was 7.92MPa. After the completion of the bridge, the stress values at the upper edge were 7.35MPa, and at the lower edge were 7.93MPa. The results complied with the specification requirements, indicating that the structure was in a safe condition.

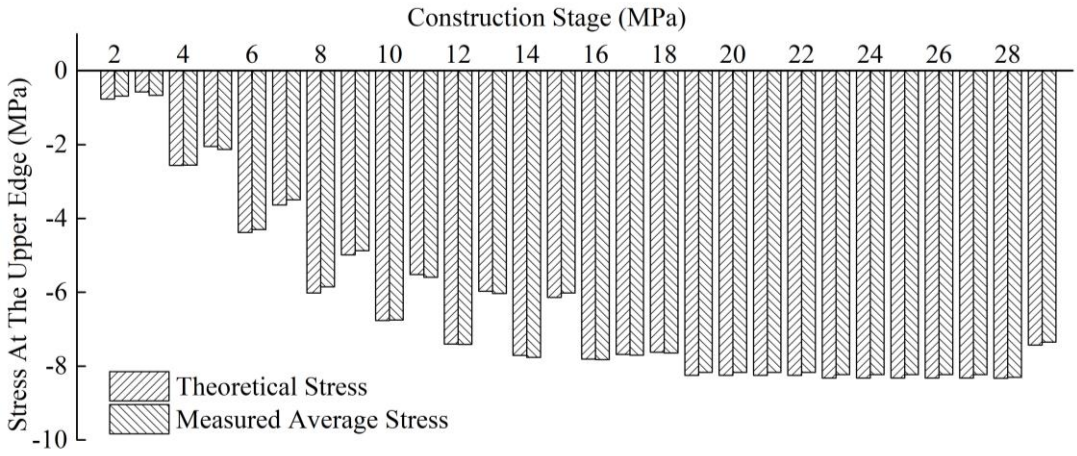

Fig. 15 – Comparison chart of upper edge stress

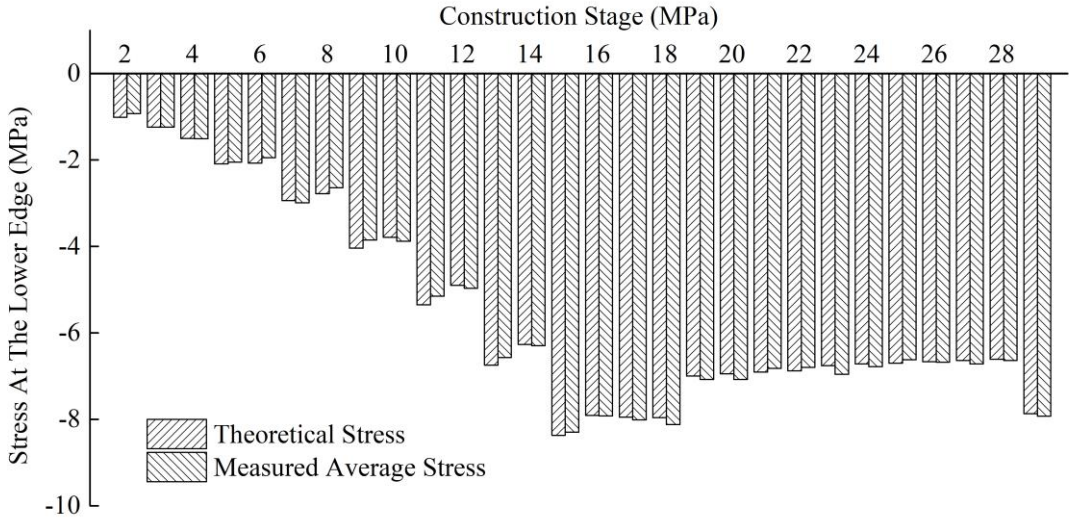

Fig. 16 – Comparison chart of lower edge stress

Monitoring results of stress at midspan

Taking the midspan section of 2# span as an example, as shown in Figure 17 and Figure 18. During the structural system transformation, the measured stress variation trend is consistent with the theoretical trend, with an error range of -0.2MPa to 0.17MPa, meeting the specifications requirements. During the pouring of segment A8 of 1# span, a tensile stress of 0.56MPa appeared at the upper edge of the midspan of 2# span. This tensile stress is a temporary stress effect during the construction stage, which will disappear in later stages and its magnitude meets the specification requirements, not affecting the safety performance of the entire construction process. After the completion of the second phase of bridge paving, the stress at the upper edge of the midspan of 2# span is -1.66MPa, with an error of 0.03MPa, and the stress at the lower edge is -10.39MPa, with an error of 0.09MPa, indicating that the structure meets design and specification requirements.

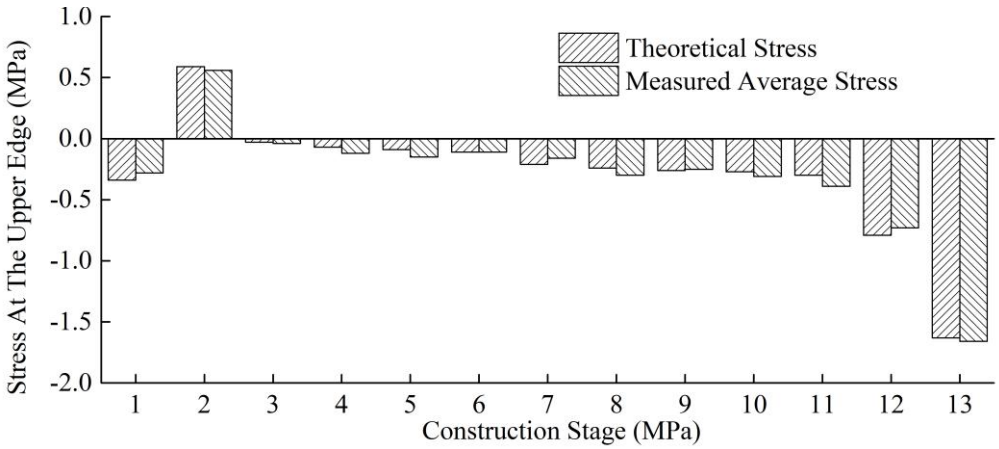

Fig. 17 –Comparison chart of upper edge stress

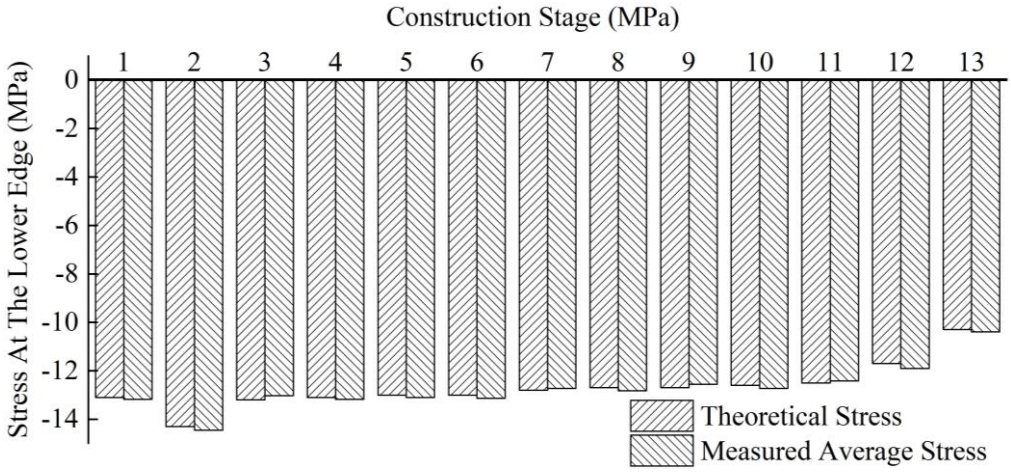

Fig. 18–Comparison chart of lower edge stress

CONCLUSION

This paper takes the prestressed concrete continuous beam bridge of the 13th span as the background and conducts monitoring and analysis in conjunction with the actual construction process. The main work conducted and the conclusions drawn are as follows:

(1) Taking the overhang pouring process of Pier 2# as an example for engineering alignment control, the results show that the deflection deformation of the bridge during various construction stages is essentially consistent with the theoretical calculations. In the final bridge completion stage, the alignment conforms to the design requirements. The construction monitoring work has achieved good results in terms of alignment.

(2) Using grey system theory to predict errors and adjust the deflection of beam segments during cantilever construction, a comparison and analysis of different prediction methods were conducted. The results show that both BP neural network and grey system theory have achieved good results in predicting the deflection of long-span prestressed concrete continuous beam bridges in the maximum cantilever state.

(3) Taking the root and mid-span sections of a certain cantilever as an example for stress monitoring, a comparison was made between the theoretical stress and actual stress throughout the construction process. The results show that the root of the cantilever experienced compressive

stress during the entire construction process, with the measured values closely matching the theoretical values. At the mid-span upper section, a temporary tensile stress of 0.56MPa occurred during the construction process, while other stages exhibited compressive stress, with the measured values closely approximating the theoretical values. The entire monitoring process achieved good results in terms of stress monitoring.

REFERENCES

[1] ZHANG, Chunyu, et al. Seismic reliability research of continuous girder bridge considering fault-tolerant semi-active control [J]. Structural Safety, 2023, 102: 102322.
[2] WU, Bitao, et al. Damage identification method for continuous girder bridges based on spatially-distributed long-gauge strain sensing under moving loads [J]. Mechanical Systems and Signal Processing, 2018, 104: 415-435.
[3] CHENG, Xiao-Xiang. Model updating for a continuous concrete girder bridge using data from construction monitoring [J]. Applied Sciences, 2023, 13.6: 3422.
[4] ZHENG, Shangmin, et al. Semi-active control of seismic response on prestressed concrete continuous girder bridges with corrugated steel webs [J]. Applied Sciences, 2022, 12.24: 12881.
[5] Yang Z , Ping Z , Zhu Y , et al. NC-UHPC Composite Structure for Long-Term Creep-Induced Deflection Control in Continuous Box-Girder Bridges[J]. Journal of Bridge Engineering, 2018, 23(6).
[6] Lounis Z , Cohn M Z . Optimization of Precast Prestressed Concrete Bridge Girder Systems[J]. Pci Journal, 1993, 38(4):60-78.
[7] Wang J . Constructing linear control of continual beam bridge cantilever pouring in railway passenger traffic special line[J]. Shanxi Architecture, 2008.
[8] XU, Changjie; XU, Lige; ZHOU, Jian. Integral lifting of a three-span continuous beam bridge [J]. Journal of Performance of Constructed Facilities, 2015, 29.4: 04014117.
[9] HUANG, Fu Wei, et al. Analysis on attenuation-amplification effect and vibration monitoring of pier-beam of continuous beam bridge under near blasting [J]. Applied Mechanics and Materials, 2013, 353: 1919-1922.
[10] LUO, Lanxin, et al. Finite element model updating method for continuous girder bridges using monitoring responses and traffic videos [J]. Structural Control and Health Monitoring, 2022, 29.11: e3062.
[11] LIANG, Ruijun, et al. Multiple tuned inerter-based dampers for seismic response mitigation of continuous girder bridges [J]. Soil Dynamics and Earthquake Engineering, 2021, 151: 106954.
[12] Chen S . The Test Research of Stress Monitoring in Construction Stage of WuZhong Yellow River Bridge[J]. Proceedings of the National Academy of Sciences, 2005, 80(15):4842-6.
[13] Zhang H , Yang B , Huang S . Dynamic geometry monitoring system and its application in Sutong Bridge construction[J]. Geo-spatial Information Science, 2010, 13(002):137-143.
[14] Krontal, Ludolf, Tamms, et al. Monitoring of bridge structures as a tool of construction supervision[J]. Bautechnik, 2015, 92(2):123-133.
[15] Sthler S C , Sens-Schnfelder C , Niederleithinger E . Monitoring stress changes in a concrete bridge with coda wave interferometry[J]. The Journal of the Acoustical Society of America, 2011, 129(4):1945-1952.
[16] Saman, Farhangdoust, Armin, et al. Health Monitoring of Closure Joints in Accelerated Bridge Construction: A Review of Non-Destructive Testing Application[J]. Journal of Advanced Concrete Technology, 2019, 17(7):381-404.
[17] LIANG, Ruijun, et al. Multiple tuned inerter-based dampers for seismic response mitigation of continuous girder bridges [J]. Soil Dynamics and Earthquake Engineering, 2021, 151: 106954.
[18] ZHANG, Lu, et al. Reference-free damage identification method for highway continuous girder bridges based on long-gauge fibre Bragg grating strain sensors [J]. Measurement, 2022, 195: 111064.
[19] ZHANG, X. Y., et al. Endowing BIM Model with Mechanical Properties--Finite Element Simulation Analysis of Long-Span Corrugated Steel Web Continuous Beam Bridge [J]. In: Journal of Physics: Conference Series. IOP Publishing, 2022: 012006.